THE JOURNAL OF PHYSICAL CHEMISTRY B

Article

pubs.acs.org/JPCB

Association of Small Hydrophobic Solute in Presence of the Osmolytes Urea and Trimethylamine-*N*-oxide

Rahul Sarma and Sandip Paul*

Department of Chemistry, Indian Institute of Technology, Guwahati Assam, India 781039

ABSTRACT: Influences of two naturally occurring osmolytes, urea and trimethylamine-*N*-oxide (TMAO), on hydrophobic interactions of methane are investigated by performing molecular dynamics (MD) simulations. In this study, we have used two different models of methane: one is of single united site (UA), and the other contains 5-sites (AA). We observe that two methane models behave similarly in pure water and in aqueous osmolyte solutions except for the fact that AA model of methane behaves slight differently in aqueous binary urea solution. Our potentials of mean force (PMF) calculations followed by association constant estimation and cluster structure analyses suggest urea-induced enhancement of methane association for the methane AA model. For both models, we observe the dehydration of methane molecules in presence of osmolytes. We also find the collapse of the second shell of water by urea and water structure enhancement by TMAO molecules. Our preferential interaction parameter calculations show that in binary aqueous urea solution methane molecules are expelled by urea molecules and this effect is more pronounced for the AA model. On the other hand, in binary aqueous TMAO solution, methane prefers to interact more with TMAO than water. Our water orientational structure calculations show that the orientation of water molecules near to hydrophobic moiety is anisotropic and osmolytes have a negligible effect on it. We also observe the osmolyte-induced water−water hydrogen bond lifetime increase in the hydration shell of methane as well as in the subsequent layers.

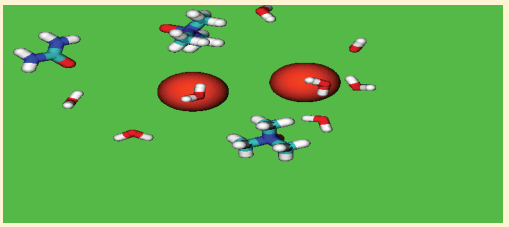

I. INTRODUCTION

It is known that the stability of native proteins in aqueous solution is a result of the balance between protein−water and intraprotein interactions, and perhaps it is not surprising that the protein stability is sensitive to surrounding chemical environments. In particular, it has been known for many years that a high concentration of urea, which is one of the most commonly available osmolytes (small solutes used by cells to maintain cell volume), can cause the denaturation of protein in solutions[1] and hence can inhibit many important biological processes. To adapt to this harsh chemical environment, organisms generally accumulate some osmolytes that counteract protein perturbation induced by urea. Of these counteracting osmolytes, TMAO is among the most potent and has attracted particular attention in recent years.[1−4] There is now good evidence that, at about a 2:1 urea/TMAO ratio, the denaturing effect of urea is nullified by TMAO and more interestingly, this is the ratio generally found in tissues containing high urea levels.[5,6] The mechanism by which urea denatures protein and TMAO counteracts this denaturation is an important question in protein science, and great strides have been made in this direction both experimentally and theoretically in the last several decades. However, the molecular mechanisms are still not well-understood. Two possible mechanisms[1,7−13] for urea-induced denaturation have been proposed: (a) alteration of water structure by urea to enhance hydration of protein and (b) direct interaction of urea with protein. These possible mechanisms are not mutually exclusive, and both could contribute to urea-induced denaturation. On the other hand, the proposed mechanisms by which TMAO counteracts urea-induced protein denaturation are through enhancement of water−water and water−urea interactions and also through direct interaction with water and urea and thereby preventing them to solvate protein.[2,12−16]

In view of the importance of side-chain hydrophobic interactions in the stability of proteins, and since the molecular mechanism of the effects of the osmolytes urea and TMAO on protein structure remains elusive due to complex interactions among solvent, osmolytes, and different groups of proteins, to mimic the hydrophobic interactions, the hydration of simple hydrophobic molecules in the presence of osmolytes has been studied extensively. Although many recent studies have been devoted to understanding the effects of urea and TMAO on hydrophobic interactions in aqueous solution, all facets of it are not completely understood to this date. Wallqvist et al.[17] performed molecular dynamics (MD) simulations to assess the effect of urea on the hydrophobic interaction between a methane pair. Their calculations of potentials of mean force (PMF) showed that urea actually enhances hydrophobic interaction, in contradiction to the hypothesis that urea preferentially solvates the hydrophobic residues.[18] Urea-induced enhancement of methane−methane association was reported in other MD simulation studies also.[19,20] Oostenbrink and Van Gunsteren,[21] on the other hand, studied the aggregation of methane in water and the effect of urea on hydrophobic clustering by simulation for 13 systems of

Received: October 31, 2011
Revised: January 29, 2012
Published: February 2, 2012

different sizes and compositions. Their simulations showed that a high urea concentration does not reduce hydrophobic interaction; rather it enhances slightly the clustering of methane molecules. In contrast to this small solute, hydrophobic interactions of larger solutes are believed to be destabilized by urea.[20,22] Trzesniak et al.[20] examined solvation free energies of six aliphatic hydrocarbons by using MD simulations and found that, for hydrocarbons larger than methane, transfer is favorable from water to 6.9 M urea. More recently, Lee and Van der Vegt[22] investigated the PMF between a neopentane pair in water and in aqueous solution of urea. Their results showed significant stabilization of the solvent-separated configuration of neopentane relative to the associated state in aqueous urea as compared to water. Further studies from Zangi et al.[23] showed that a chain of purely hydrophobic groups undergoes a structural transition from folded to unfolded states upon the addition of urea. With regard to TMAO-induced hydrophobic interactions, Athawale et al.[24] investigated the effects of TMAO on the thermodynamics of hydrophobic hydration and interactions of small solutes as well as on the folding−unfolding conformational equilibrium of a hydrophobic polymer in water. The major conclusion of their study was that TMAO has a negligible effect either on the thermodynamic stability of contact and solvent-separated conformations relative to pure water. They argued that the neutrality of TMAO toward hydrophobic interactions is due to lacking of strong preferential binding or depletion of TMAO in the vicinity of hydrophobic solutes and due to the precise balance of the effects of its hydrophobic methyl groups and hydrophilic N═O group. The preferential solvation model where water and urea prefer to make strong hydrogen bonds with TMAO (rather than protein) which leads to the inhibition of unfolding and disruption of neopentane association by TMAO was also reported in the literature.[14,25,26]

As discussed above, there have been many simulation studies that investigate the interaction of methane in aqueous urea and TMAO solutions. However, the effects of ternary urea−TMAO−water mixtures on methane−methane interactions are yet to be addressed. Moreover, to the best of our knowledge, the influences of urea and TMAO on the orientational distribution and hydrogen-bond properties and dynamics of water molecules at discrete distances from the solute methane have not been investigated so far. In this article, we therefore, describe the solvation characteristics of methane molecules in aqueous solutions containing the osmolytes urea and TMAO as well as in binary aqueous osmolyte solutions. Again, one interesting observation concerning the solvation of hydrophobic solute is somewhat less layering of solvent density around nonspherical hydrophobic solutes.[20,27] Because of the important role of solvent molecules on hydrophobic interactions, model dependency of hydrophobic interaction in aqueous solution can be expected. Previous MD studies of hydrophobic solute in water also showed that the association of the solute is influenced by the model of the solute used. In particular, Lee and Van der Vegt observed that, in TIP4P water, the contact minimum of neopentane was significantly deeper for the five-site model than that for the single-site Lennard−Jones (LJ) neopentane model.[22] Besides this, there have also been studies of length-scale-dependent hydrophobicity.[28−30] These findings encouraged us to consider two methane models: the united-atom (UA) and all-atom (AA) models. Hydrogen atoms attached to the carbon atom are implicit for the UA model while explicit for the AA model. Our goal was to get a better idea of model dependencies of hydrophobic interactions in the aqueous chemical environment. We first examine whether urea or TMAO has any significant effect on the aggregation of methane in aqueous solution. To study the aggregation of methane in aqueous solutions, we calculate the PMF and then analyze the average cluster size in the system. An insight picture of the influences of these two osmolytes on aggregation is obtained by examining their effects on the water structure and also their direct interactions with the hydrophobic solute. The familiar water oxygen−oxygen radial distribution function (rdf) is used to describe water structuring, and coordination number calculation and Kirkwood−Buff analysis of solute−solvent rdfs are used to examine the preferential binding with the solute. Furthermore, we investigate the orientation of solvent/cosolvent with respect to the hydrophobic solute and analyze the hydrogen-bonding interaction of water in the presence of osmolyte. In the second part of this article, we focus on the orientational distribution and the hydrogen-bond properties and dynamics of water molecules around different regions of a single methane particle to describe water−water hydrogen bonding and to quantify the extent of water structuring at discrete distances from the solute. The influence of urea and TMAO on hydrogen bond dynamics is also discussed in this section.

The remainder of this article is organized into three sections. The models and simulation details are briefly described in section II; results are discussed in section III, and our conclusions are summarized in section IV.

II. MODELS AND SIMULATION METHOD

To study the effects of urea and TMAO on hydrophobic interactions of methane, we have carried out classical MD simulations in four different solvent systems: pure water, aqueous urea, aqueous TMAO, and mixed urea/TMAO. The number of molecular species considered in different systems are listed in Table 1. Note that, for water orientational profile calculations (as well as for water−water hydrogen bond properties and dynamics calculations), we have used a single solute molecule immersed in water (and osmolytes), and to keep the total number of molecules constant, we replaced nine methane solutes by water molecules. In all of the simulations, the extended simple point-charge (SPC/E) model[31] was used for water, the so-called Duffy−Kowalczyk−Jorgensen (DKJ) model[32] was adopted for urea, and TMAO was described with a rigid version of model proposed by Kast et al.[33] Two different

Table 1. Overview of Simulations[a]

model	system	V (nm^3)	N_s	N_u	N_t	N_w	M_u	M_t
united atom (UA)	$S_{UA,1}$	15.21	10	0	0	490	0	0
	$S_{UA,2}$	19.51	10	100	0	390	8.51	0
	$S_{UA,3}$	18.07	10	0	40	450	0	3.68
	$S_{UA,4}$	22.36	10	100	40	350	7.43	2.97
all atom (AA)	$S_{AA,1}$	15.39	10	0	0	490	0	0
	$S_{AA,2}$	19.46	10	100	0	390	8.53	0
	$S_{AA,3}$	17.77	10	0	40	450	0	3.74
	$S_{AA,4}$	22.25	10	100	40	350	7.46	2.98

[a]Numbers in system names are used for the identification of methane in water (1), aqueous urea (2), aqueous TMAO (3), and mixed urea/TMAO (4) solutions. V, N, and M represent box volume, number of molecules, and molar concentration, respectively. s, w, u, and t refer to solute (methane), water, urea, and TMAO.

dx.doi.org/10.1021/jp2104402 | J. Phys. Chem. B 2012, 116, 2831−2841

models were used for methane: a single-site united-atom (UA) model[34] and 5-site (AA) model.[35] All models employed were rigid, and the interaction between atomic sites of two different molecules is expressed as

$$u_{\alpha\beta}(r_{\alpha\beta}) = 4\varepsilon_{\alpha\beta}\left[\left(\frac{\sigma_{\alpha\beta}}{r_{\alpha\beta}}\right)^{12} - \left(\frac{\sigma_{\alpha\beta}}{r_{\alpha\beta}}\right)^{6}\right] + \frac{q_\alpha q_\beta}{r_{\alpha\beta}} \quad (1)$$

where $r_{\alpha\beta}$ is the distance between atomic sites α and β, and q_α is the charge of the site α. The LJ parameters $\sigma_{\alpha\beta}$ and $\varepsilon_{\alpha\beta}$ were obtained by using the combining rules $\sigma_{\alpha\beta} = (\sigma_\alpha + \sigma_\beta)/2$ and $\varepsilon_{\alpha\beta} = (\varepsilon_\alpha\varepsilon_\beta)^{1/2}$. The values of the LJ parameters and the partial charges for methane, urea, TMAO, and water are summarized in Table 2.

Table 2. Lennard–Jones Parameters and Charges Used in the Models Considered[a]

	atom type	σ (Å)	ε (kJ/mol)	charge (e)
water	O_w	3.166	0.646	−0.8476
	H_w			0.4238
urea	C_u	3.75	0.4365	0.142
	O_u	2.96	0.873	−0.390
	N_u	3.25	0.7067	−0.542
	H_u	0.0	0.0	0.333
TMAO	C_t	3.041	0.281	−0.26
	N_t	2.926	0.8314	0.44
	O_t	3.266	0.6344	−0.65
	H_t	1.775	0.0769	0.11
methane (UA)	me	3.70	1.234	0.0
methane (AA)	C	3.50	0.276	−0.24
	H	2.5	0.1261	0.06

[a] e is the elementary charge.

The solution properties were investigated by carrying out MD simulations at 298 K. All calculations have been performed with 500 total molecules in a cubic box of length L. The LJ interactions were spherically truncated at a radius of $L/2$. The long-range electrostatic interactions were treated using the Ewald method[36] with the convergence parameter $\alpha = 6.4/L$. The quaternion formulation of the equations of rotational motion was employed, and the leapfrog algorithm with a time step of 10^{-15} s was used for the time integration. In the starting configuration, the molecules were located on a face-centered-cubic lattice with random orientations. At first the MD simulations were performed in NPT ensemble to obtain the box volume corresponding to 1 atm pressure. During this initial phase of the simulation, the volume of the simulation box was allowed to fluctuate, and the average volume was determined at the end of the simulation. Subsequently, NVT ensemble simulations were carried out using the box length obtained from the previous NPT simulation run. NVT MD runs of 5 ns were used to equilibrate each system. During the equilibration, the velocities were rescaled to fix the temperature. Finally, each system was run for a further 10 ns using the NVT MD method,[36] and these are the results reported.

III. RESULTS AND DISCUSSION

A. Methane–Methane Pair Potentials of Mean Force. To calculate PMF, we have used methane–methane pair correlation functions, $g_{ss}(r)$, in the relation

$$W(r) = -k_B T \ln g_{ss}(r) \quad (2)$$

where k_B is the Boltzmann constant and T is the temperature.

In Figure 1 we have shown methane–methane PMFs of each methane model for all four systems simulated here. The PMF curves reveal the existence of contact and solvent-separated configurations with the contact minimum (CM) is having higher well depth than that of the solvent-separated minimum (SSM). The maximum between the two minima is known as the desolvation barrier. From Figure 1, we find that, in absence

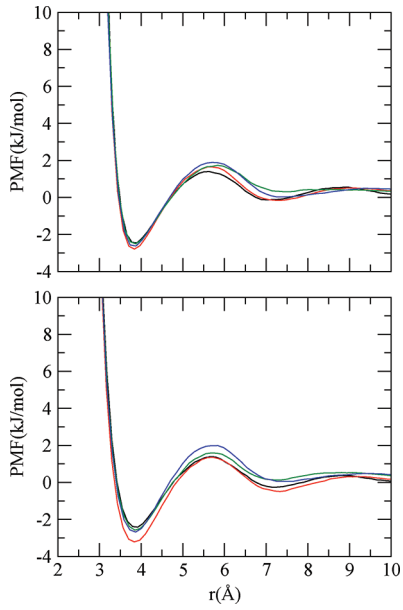

Figure 1. PMF for UA (top) and AA (bottom) models of methane in water (black), aqueous urea (red), aqueous TMAO (green), and mixed urea/TMAO (blue) solutions. The estimated standard deviations for all systems vary from 0.1 to 0.22 kJ/mol.

of osmolytes, the CM, the barrier, and the SSM appear at about 3.9, 5.6, and 7.0 Å, respectively. The two models of methane have similar depths of the CM and the SSM and also have a similar height of the desolvation barrier. Focusing on the effect of urea on methane–methane interaction, we find that, for the UA model, the CM and the SSM are only slightly modified in the presence of urea. The main influence of urea on PMF is to increase the barrier height of the PMF. For the AA model, the effect of urea on the CM and the SSM is more pronounced, making these two minima deeper as compared to pure water. For both models of methane, TMAO, on the other hand, increases the depth of the CM slightly, but shifts the barrier and the SSM of the PMF upward in both aqueous TMAO and mixed urea/TMAO solutions.

To understand the extent of association of methane in pure water and the effect of urea and TMAO on it, we have calculated the association constant, K_a, by integrating the PMF to the first maximum (the barrier) which defines the outer limit of the solute–solute contact configuration. The K_a is defined as

$$K_a = 4\pi \int_0^{r_a} r^2 e^{-W(r)/k_B T} dr \quad (3)$$

where r_a is the position of the barrier in the corresponding PMF curve. We note that higher the value of K_a, greater will be the association of the hydrophobic solute in solution. Any perturbation that increases the value of K_a will, therefore, favor the associated state of the solute. The values of K_a for

dx.doi.org/10.1021/jp2104402 | J. Phys. Chem. B 2012, 116, 2831–2841

different systems simulated here are presented in Table 3. From this table we observe that, except for the system $S_{AA,2}$, the effect of osmolytes urea and TMAO on the association of methane is almost negligible.

Table 3. Association Constants (K_a) for Hydrophobic Solutes in Aqueous Solutions

methane (UA)		methane (AA)	
system	K_a (M^{-1})	system	K_a (M^{-1})
$S_{UA,1}$	0.44	$S_{AA,1}$	0.47
$S_{UA,2}$	0.46	$S_{AA,2}$	0.59
$S_{UA,3}$	0.47	$S_{AA,3}$	0.48
$S_{UA,4}$	0.44	$S_{AA,4}$	0.48

B. Cluster Structure Analysis. To quantify the clustering of hydrophobic methane molecules in pure water and as well as in the presence of osmolytes, we have estimated the average cluster size in our systems. We adopted the method first proposed for LJ fluids by Martinez et al.[37] and then successfully employed it by Kokubo and Pettitt[38] in their simulation study of aqueous urea solution. Each molecule can be assigned low, average, or high density clusters of its species depending upon the following relations:

$$\begin{aligned} &\text{low if} \quad n < n_0 - \delta \\ &\text{average if} \quad n_0 - \delta \le n \le n_0 + \delta \\ &\text{high if} \quad n > n_0 + \delta \end{aligned} \tag{4}$$

Note that, to calculate the number of molecules in the solvation sphere (n) excluding the reference particle, we have integrated the methane−methane pair correlation function to the first minimum (rather than considering the instantaneous number of molecules around a test molecule) and for calculating the average number of molecules (n_0) we have adopted the method proposed by Martinez et al.[37] δ is the fluctuation, and in our case we set it to 20% of the average number of molecules.

The results of our cluster structure analyses for two methane models are shown in Table 4. It is apparent from Table 4 that, for both models of methane, the difference between $n - n_0$ values are very small for both in pure water and in aqueous solutions of osmolyte. This difference is also close to the corresponding δ value indicating average sized clusters in those solutions. The average cluster size is slightly higher for the AA methane model in aqueous binary urea solution, and for other solutions the effect of osmolytes on the aggregation of methane molecules is negligible. These observations are in consistent with our estimated K_a values for different solutions discussed above.

Table 4. Methane Cluster Sizes for Different Systems[a]

system	n	n_0	δ	$n - n_0$	remark
$S_{UA,1}$	0.48	0.49	0.10	−0.01	average
$S_{UA,2}$	0.39	0.37	0.07	−0.02	average
$S_{UA,3}$	0.43	0.46	0.09	−0.03	average
$S_{UA,4}$	0.33	0.35	0.07	−0.02	average
$S_{AA,1}$	0.50	0.49	0.10	0.01	average
$S_{AA,2}$	0.50	0.40	0.08	0.10	high
$S_{AA,3}$	0.45	0.43	0.09	0.02	average
$S_{AA,4}$	0.36	0.37	0.07	−0.01	average

[a] n_0, n, and δ are the average number of methane molecules, the number of methane molecules in the first coordination shell, and the fluctuation, respectively.

C. Site−Site Radial Distribution Functions. To obtain molecular details of methane solvation, we have computed site−site rdf's between methane and the solution species (water, urea, and TMAO) and also between water molecules. To analyze the solvation of the hydrophobic solute further, we have calculated coordination numbers for water, urea, and TMAO about the hydrocarbon solute. The coordination numbers are defined as[39]

$$n_{\alpha\beta} = 4\pi\rho_\beta \int_{r_1}^{r_2} r^2 g_{\alpha\beta}(r)\mathrm{d}r \tag{5}$$

where $n_{\alpha\beta}$ represents the number of atoms of type β surrounding atom α in a shell extending from r_1 to r_2 and ρ_β is the number density of β in the system. For the calculation of first solvation shell coordination number, the typical values of r_1 and r_2 are zero and the distance of the first minimum in the corresponding distribution function, respectively.

Figure 2 displays rdfs involving methane (C for AA methane model) and the central atom of water (O_w), urea (C_u), and TMAO (N_t). Focusing on the hydration of the hydrophobic solute in the absence of osmolyte first, we find that, compared to the bulk density, the water density increases in the first and second hydration spheres around the solute. The distribution functions are similar for the two models of methane. The first peak of rdf appears at about 3.6 Å which is consistent with the formation of the SSM at about 7.0 Å in the PMF of methane in water. The first shell coordination number analysis (see Table 5) shows an average of about 20 water molecules in the first hydration shell of methane. In aqueous solution of osmolytes, due to the presence of osmolyte and also due to the reduced number density of water, the number of water molecules in the first hydration shell decreases. To nullify the effect of reduced number

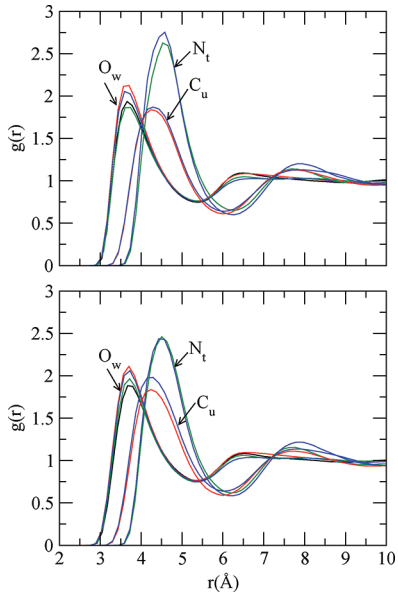

Figure 2. Solute−solvent site−site distribution functions for UA (top) and AA (bottom) models of methane in water (black), aqueous urea (red), aqueous TMAO (green), and mixed urea/TMAO (blue) solutions. Only the central atoms of water (O_w), urea (C_u), and TMAO (N_t) are considered.

dx.doi.org/10.1021/jp2104402 | J. Phys. Chem. B 2012, 116, 2831−2841

Table 5. Average Number of Water Molecules (N_w) in the First Hydration Shell of Methane

methane (UA)		methane (AA)	
system	N_w	system	N_w
$S_{UA,1}$	20.14	$S_{AA,1}$	20.10
$S_{UA,2}$	12.84 (16.03)	$S_{AA,2}$	12.75 (16.00)
$S_{UA,3}$	15.87 (18.50)	$S_{AA,3}$	16.09 (18.46)
$S_{UA,4}$	10.31 (14.39)	$S_{AA,4}$	10.32 (14.36)

density of water in the osmolyte solution, we have calculated the coordination numbers assuming that the only change with added osmolyte comes through the reduced number of water and these numbers are also given in Table 5 in parentheses. The replacement of water by osmolyte from the first hydration shell of methane is clear from these values. For urea solution, the dehydration is about 36%. TMAO, on the other hand, reduces the amount of water in the hydration sphere by about 21%. The dehydrating effect is obviously more pronounced for systems containing both urea and TMAO, with the amount of water decreased by about 49%. Moreover, we find that the ratio of the first shell water molecules in pure water and in aqueous osmolyte solution is higher than the respective ratio of water molecules present in those systems. For example, for UA model of methane, the ratio of first shell water molecules in pure water ($S_{UA,1}$) and in aqueous urea solution ($S_{UA,2}$) is 1.57:1 which is higher than the ratio of total number of water molecules present in those systems (i.e., 1.25:1). This again reveals osmolyte-induced dehydration of methane.

In Table 6, we have presented the average number of water, urea, and TMAO molecules in the solvation shell defined as being closer than 6.3 Å to the solute. From this table, we find that for all simulated systems, as expected, the number of osmolyte molecules in the solvation shell is less than those of water molecules. For binary water−urea solution, the water/urea ratio in this cutoff region around the solute is higher than the respective ratio in the bulk (presented within parentheses). In contrast to urea, the water/TMAO ratio is lower than the respective ratio in the bulk in binary aqueous TMAO solution. Moreover, in ternary water-urea-TMAO solution, although the number of urea molecules is higher than that of TMAO molecules, the urea/TMAO ratio is slightly lower than the bulk ratio. These results demonstrate that in its solvation shell, methane prefers TMAO molecules only slightly over both water and urea molecules. But, we note that the magnitude of enhancement of TMAO concentration in the vicinity of hydrophobic methane is marginal. The depletion or enhancement of solution species near a solute are calculated by examining the preferential solvation of methane discussed below.

Table 6. Average Number of Water (N_w), Urea (N_u), and TMAO (N_t) Molecules in the Solvation Shell of Methane Defined as Being Closer than 6.3 Å to the Solute[a]

system	N_w	N_u	N_t	N_w/N_u	N_w/N_t	N_u/N_t
$S_{UA,2}$	20.26	4.65		4.36 (3.90)		
$S_{UA,3}$	25.36		2.53		10.02 (11.25)	
$S_{UA,4}$	15.50	4.21	2.01	3.68 (3.50)	7.71 (8.75)	2.10 (2.50)
$S_{AA,2}$	20.17	4.58		4.40 (3.90)		
$S_{AA,3}$	25.52		2.42		10.55 (11.25)	
$S_{AA,4}$	15.50	4.36	1.85	3.56 (3.50)	8.38 (8.75)	2.36 (2.50)

[a]The bulk ratios are presented within parentheses.

Preferential Solvation. Preferential solvation or preferential interaction is the measure of deviations from an ideal solvation model. Following Ben-Naim,[40] it can be defined as

$$\delta_{\alpha\beta} = x_{\alpha\beta}(r) - x_\alpha = \frac{x_\alpha x_\beta (G_{\alpha\beta} - G_{\beta\beta})}{x_\alpha G_{\alpha\beta} + x_\beta G_{\beta\beta} + V_c} \quad (6)$$

where $x_{\alpha\beta}$ (r) is the local mole fraction and it is defined as the number of α molecules divided by the total number of molecules present in a sphere (of radius r) around a β molecule and x_α is the total mole fraction of α molecule. So, $\delta_{\alpha\beta}$ measures the local mole fraction minus total mole fraction. V_c is the volume with radius r and $G_{\alpha\beta}$ is called the Kirkwood−Buff G factor. $G_{\alpha\beta}$ is calculated using rdf, $g_{\alpha\beta}(r)$, as[20,21]

$$G_{\alpha\beta} = 4\pi \int_0^\infty r^2[g_{\alpha\beta}(r) - 1]dr \quad (7)$$

We calculated the excess coordination number, $N_{\alpha\beta}$ from the density-weighted integral as

$$N_{\alpha\beta} = 4\pi\rho_\alpha \int_0^\infty r^2[g_{\alpha\beta}(r) - 1]dr \quad (8)$$

In eq 8, $4\pi\rho_\alpha r^2 g_{\alpha\beta}$ (r) estimates the average number of α molecules around a β molecule in a spherical shell of width dr at radius r and $4\pi\rho_\alpha r^2 dr$ measures (ideal) average number of α molecules in a spherical shell. So, $N_{\alpha\beta}$ represents excess number of α molecules around a β molecule. Since $g_{\alpha\beta}$ (r) goes to unity at large distances, eq 8 can be written as,

$$N_{\alpha\beta} \approx 4\pi\rho_\alpha \int_0^{r_c} r^2[g_{\alpha\beta}(r) - 1]dr \quad (9)$$

where the upper integration limit, r_c, is the radius of a correlation volume in which the solution structure differs from that in the bulk and thus $g_{\alpha\beta}$ (r) differs from unity. A positive value of $N_{\alpha\beta}$ suggests the enhancement of molecule α around a β molecule, while a negative value indicates its depletion. Note that in these calculations r_c is sufficiently large so that beyond which the correlations are small giving rise to $g_{\alpha\beta}$ $(r) \approx 1$.

Figure 3 shows the $N_{\alpha\beta}$ values for water (O_w), urea (C_u), and TMAO (N_t) about methane as a function of integration distance. We find that, for aqueous binary urea solution, the $N_{\alpha\beta}$ value for urea is lower than that for water and this effect is much more pronounced for the all site methane model. This is probably due to the fact that urea repels methane molecules and the latter are driven in to water solvation. As a result, this leads to the enhancement of methane concentrations, and thereby the formation of methane clusters takes place. These observations are in consistent with our calculated K_a values discussed above. We note that urea-induced enhancement of hydrophobic interactions between methane molecules is also reported previously.[20,21] On the other hand, in binary aqueous solutions of TMAO, methane molecules prefer to interact more with TMAO molecules than water molecules. Because of these preferential methane−TMAO interactions, one would expect reduced hydrophobic interactions among the methane molecules and the decrease of association constant value K_a

dx.doi.org/10.1021/jp2104402 | J. Phys. Chem. B 2012, 116, 2831−2841

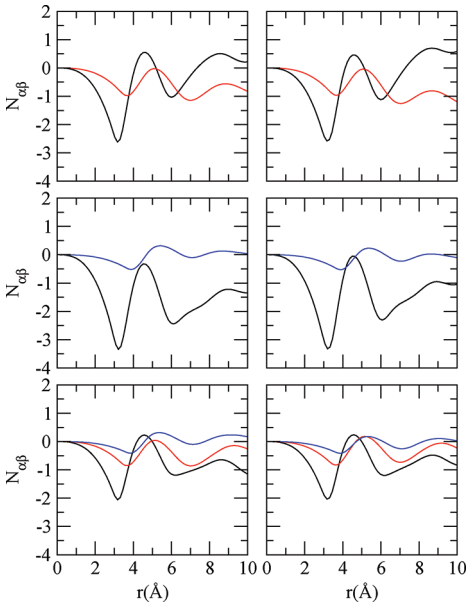

Figure 3. Kirkwood–Buff excess coordination number, $N_{\alpha\beta}$, for water (black), urea (red), and TMAO (blue) about methane in aqueous solutions of urea, TMAO, and mixed urea/TMAO (from top to bottom, respectively) as a function of distance. The left panel is for the UA model of methane, and the right panel is for the AA model.

thereby leading to the solvation of methane molecules. But, our calculated K_a values for these solutions show the negligibly small effect of TMAO on methane association. We note that in the PMF curve the contact minimum (CM) between two methane molecules appears at 3.9 Å and the first peak of methyl–methyl distribution function of TMAO molecules (not shown) appears at 3.7 Å. The closeness of these two distances suggests that hydrophobic methane molecules are congruent with methyl groups of TMAO and can act as a substitute for the methyl group of TMAO molecules. So, TMAO molecules help to associate methane molecules. These two opposing effects, one is the decrease of hydrophobic interactions due to interactions with the methyl groups and the other is the increase of association of methane molecules due to presence of methyl groups in TMAO, cancel each other, and we observe negligible effects of TMAO molecules on the methane association. For ternary water–urea–TMAO solution, the almost similar $N_{\alpha\beta}$ values for water, urea, and TMAO demonstrate that there is practically no preference for methane molecules to interact with different solvent–cosolvent species.

To evaluate possible effects of urea and TMAO on water structure, which provides details of osmolyte effect on methane hydration, we have examined water–water ($g_{O_wO_w}$) rdf in water and in solutions of osmolyte. These are shown in Figure 4. The first and second peaks, which characterize the hydrogen-bonded first neighbor and the tetrahedrally located second neighbor, appear at about 2.8 and 4.5 Å respectively, as observed previously by Wei et al.[12] Both urea and TMAO enhance the first peak, and while urea leads to a shallower first valley and a less pronounced second peak, TMAO makes the first valley deeper and the second peak more pronounced. Such changes in the O_w–O_w rdf have been used as supporting evidence for a slight second-shell collapse of water structure by urea and water-structure enhancement by TMAO.[12,13] We note that peak heights and peak positions of the O_w–O_w distribution function for pure water and binary aqueous TMAO solution are

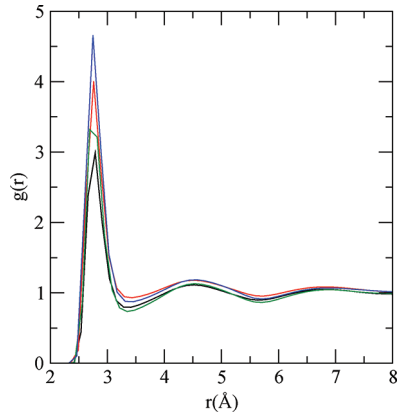

Figure 4. Water oxygen–water oxygen rdfs for the UA model of methane in water (black), aqueous urea (red), aqueous TMAO (green), and mixed urea/TMAO (blue) solutions.

in good agreement with that reported by Athawale et al.[24] We also observe the peak height enhancement of the O_w–O_w distribution function on the addition of urea into aqueous TMAO solution.

We have examined the orientation of water and osmolyte near the methane moiety by computing selective rdfs involving methane, water, urea, and TMAO. These distribution functions are shown in Figure 5 for the mixed osmolyte solution.

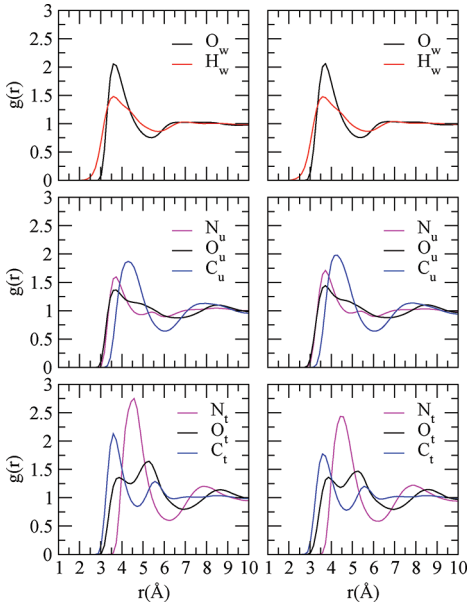

Figure 5. Solute–solvent site–site distribution functions for water, urea, and TMAO (from top to bottom, respectively) in the mixed urea/TMAO solution. The left panel is for the UA model of methane, and the right panel is for the AA model.

As reported previously,[41–44] we too observe the first peaks in O_w and H_w profiles at similar positions, supporting the parallel water orientation at the surface of a hydrophobic solute. The tail of hydrogen density at shorter separations reflects a slight preference of water hydrogens to come closer to the surface. We note that the general behavior of these distribution functions is qualitatively similar for both methane models. For O_u and N_u, the rdf profiles show the first peak at similar locations with the N_u rdf consisting of a shoulder at a longer distance. These observations suggest a side-on orientation of

dx.doi.org/10.1021/jp2104402 | J. Phys. Chem. B 2012, 116, 2831–2841

urea near the methane surface. One $-NH_2$ group of urea is directed outward, and the broad first peak of oxygen indicates a slight tendency of this site to be pointed away from the solute methane molecule. For solute−solvent rdfs involving TMAO, the C_t profile demonstrates a first peak containing two maxima separated by a dip. The peak positions suggests the preference of TMAO methyl groups near the methane moiety. It is also interesting to observe nonzero oxygen density at shorter separations with a short-range shoulder to the first peak. These findings reveal that TMAO molecules prefer a side-on orientation near the methane surface. The split carbon peak suggests that structures with at least one methyl group canted outward away from methane. So a TMAO molecule appears like a short amphiphile, and it allows the polar oxygen atom to form favorable hydrogen bonds with water and urea and also to maintain some hydrophobic contacts with the surface. Our estimated orientational preferences of different atomic sites of urea and TMAO around a hydrophobic methane are consistent with previously reported results for the neopentane united atom model.[26]

To understand the hydrogen-bonding interactions among water, urea, and TMAO, we have calculated the relevant rdfs, and the results are shown in Figure 6. Two points are worth

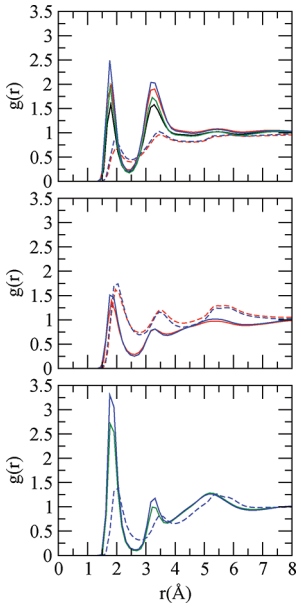

Figure 6. Hydrogen bonding involving O-atoms of water, urea, and TMAO (from top to bottom, respectively) for the UA model of methane in water (black), aqueous urea (red), aqueous TMAO (green), and mixed urea/TMAO (blue) solutions. Solid and dashed lines represent water and urea hydrogens.

noting from this figure. First, in hydrogen bonding with water, urea is a better acceptor than a donor as indicated by the stronger peaks in the O_u-H_w rdf relative to those in O_w-H_u rdf. Second, the location of the first peak reveals that TMAO can accept hydrogens from both water and urea. The stronger peaks in O_t-H_w rdf also suggest a much higher tendency of TMAO to accept hydrogens from water than from urea. To get insight into the nature of hydrogen bonding, we have calculated the first shell coordination numbers (which gives the average number of hydrogen-bonded neighbors) of different pairs of species for all simulated systems. Table 7 presents these numbers for systems containing UA methane. We note that in pure water, each water molecule has about 3.9 hydrogen-bonded neighbors. The number reduces in the presence of osmolytes, but the decrease in the number of hydrogen-bonded water molecules in the osmolyte solution is compensated by hydrogen bonding with osmolytes, and the total number of hydrogen-bonded species per water molecule remains almost unchanged. Again, from Table 7 we observe that both urea and TMAO contain an average of about three hydrogen-bonded water molecules in the binary solutions. In the mixed osmolyte solution, some water molecules around TMAO are replaced by urea. The data shows that on average there are 0.88 urea molecules that donate H-atoms to TMAO oxygen. Because of this interaction, the average number of urea−urea hydrogen bonding decreases in the presence of TMAO (the number reduces from 3.12 to 2.80).

D. Orientational Distributions. It is known that the orientational symmetry of bulk water breaks in the presence of liquid−solid or liquid−vapor interfaces.[45−48] Because water losses its orientational symmetry near the solute surface, our interest is to monitor the orientation of water molecules with respect to their distances from the hydrophobic methane center of mass and how the presence of osmolytes influence this distribution. To see this, we have calculated the distribution function of the angle formed (θ) between water dipole vector ($\hat{\mu}$) and the unit vector ($\hat{\mathbf{u}}$) pointing from the oxygen atom of water toward the center of the methane molecule (see Figure 7). We have studied the water orientational distribution around methane in three different regions of width 1 Å each depending on the distances between water and the solute: Region I (2.5−3.5 Å), Region II (3.5−4.5 Å), and Region III (10−11 Å) for the UA model of methane. For the AA model of methane, Regions I, II, and III correspond to 2.4−3.4, 3.4−4.4, and 10−11 Å, respectively. Our aim is to see how the orientation of water molecules changes as we move away from the solute molecule. For this reason, we have considered one region (Region I) nearest to the solute molecule; the second layer is 1 Å away from Region I, and the last region is considered as the bulk portion of the simulation cell (Region III). In Figure 8, we have shown the results of the normalized probability function $P(\cos\theta)$ as a function of $\cos\theta$ for the methane UA and AA models. Focusing on the orientational distribution of water in the methane−water system first, we find that, as expected, there is no preferred orientation of water molecules far away (Region III) from the solute molecule. In the interfacial regions (Region I and II), however, the probability function is nonuniform which shows an orientational structure of interfacial water molecules near to the hydrophobic surface. Water dipoles in these regions prefer to oscillate in between +0.57 and −0.57; or, in other words, water dipoles make angles in the range 55−124° with the unit vector. With increasing the distance from the solute molecule, these distribution functions become flatter. We also find that osmolyte does not have any notable influence on the orientational distribution of water.

E. Hydrogen Bond Properties and Dynamics. Bennion and Daggett,[2] using MD simulations of a protein chymotrypsin inhibitor 2, showed that the lifetime of water−water hydrogen bonds increases significantly in the presence of TMAO and the TMAO-induced ordering of both hydration layer and bulk solvent contributes to the stabilization of protein. So, in view of the importance of the counteracting effect of TMAO through the modifications of water−water hydrogen bonding, it is of interest to closely examine the hydrogen bond properties and dynamics of water molecules in the urea/TMAO mixture. These facts encouraged us to study water−water hydrogen

dx.doi.org/10.1021/jp2104402 | J. Phys. Chem. B 2012, 116, 2831−2841

Table 7. First Shell Coordination Numbers for Atom Pairs Associated with Hydrogen Bonding[a]

system	atom pair	W–W	W–U	W-T	U–W	U–U	U-T	T-W	T-U
$S_{UA,1}$	O–H	0.97							
	H–O	0.97							
	total	3.88							
$S_{UA,2}$	O–H	0.75	0.13		0.73	0.39			
	H–O	0.75	0.19		0.49	0.39			
	total	3.00	0.90		3.42	3.12			
$S_{UA,3}$	O–H	0.86						1.33	
	H–O	0.86		0.12					
	total	3.44		0.24				2.66	
$S_{UA,4}$	O–H	0.69	0.13		0.65	0.35		1.00	0.22
	H–O	0.69	0.19	0.11	0.44	0.35	0.09		
	total	2.76	0.90	0.22	3.06	2.80	0.36	2.00	0.88

[a]W, U, and T refer to water, urea, and TMAO, respectively. Numbers are with respect to the first species, and the total is calculated by taking into account the number of hydrogen atoms in water and urea.

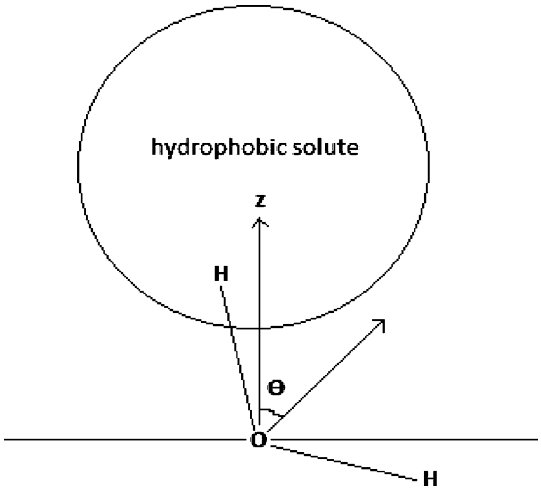

Figure 7. Angle (θ) between the dipole vector of a water molecule and the unit vector pointing from the oxygen atom of water toward the hydrophobic solute center.

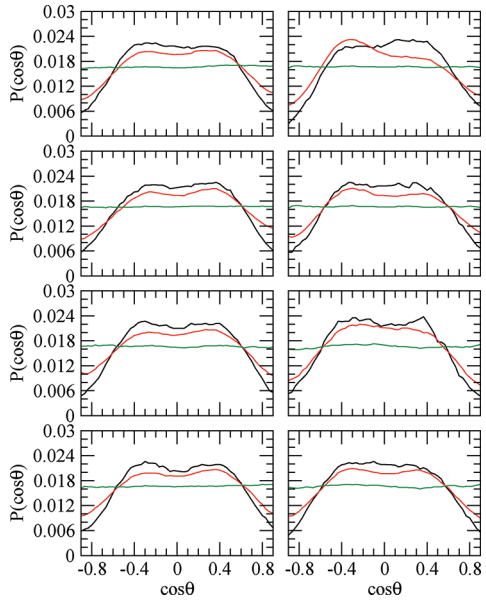

Figure 8. Orientational distribution of water for Regions I (black), II (red), and III (green) in water, aqueous urea, aqueous TMAO, and mixed urea/TMAO solutions (from top to bottom, respectively). The left panel is for the UA model of methane, and the right panel is for the AA model. Regions I, II, and III are defined in the text.

bonding in different layers around the hydrophobic solute. The regions considered were identical to those used in our orientational distribution study, and the methods and the geometric criteria for hydrogen-bond properties and dynamics calculations were described elsewhere.[14]

In Table 8, we have presented the average number (n_{HB}) of hydrogen bonds per water molecule together with the energy and lifetime of these bonds. We do not find any significant change in the average number and lifetime of hydrogen bonds with distance. However, the hydrogen bonds are slightly more attractive in the vicinity of methane (by about 1 kJ/mol) as compared to the bulk region. The negligible change in water–water hydrogen bond number indicates that methane can easily fit into the cavities generated by normal fluctuations in the solvent density without disturbing water–water hydrogen bonding. The addition of urea and/or TMAO reduces the average number of hydrogen-bonded water molecules with a slight change in energy. Osmolytes, particularly TMAO, however, enhance the lifetime of water–water hydrogen bonds. For example, for UA methane model, the lifetime increases from 1.38 ps in methane–water system to 1.88 ps in methane–water–TMAO system and then to 2.04 ps in the mixed urea–TMAO mixture. Corroborative evidence for osmolyte-induced enhancement of the water–water hydrogen bond lifetime can be seen in Figure 9, which illustrates slower relaxation of the water–water hydrogen bond correlation function (S_{HB}) with time in aqueous solutions of osmolyte. We note that our observation of the enhancement of hydrogen bonds in the presence of TMAO is in qualitative agreement with that reported by Bennion and Daggett.[2]

The variation of fraction of molecules (f_n) with n number of water–water hydrogen bonds in the simulation systems for the three selected regions are shown in Figure 10. For both models of methane in pure water, most of the water molecules are three and four coordinated with relatively lower fractions of two and five coordinated water molecules. As compared to water in the bulk (region III), the fraction of lower coordinated water molecules (f_2 and f_3) increases, and that of higher coordinated water molecules (f_4 and f_5) decreases slightly in the vicinity of the solute (regions I and II), suggesting that water loses some of its identical nearest neighbors near the hydrophobic solute surface. The effect of osmolyte on water–water hydrogen bond number is dramatic, reducing the number of four and five

dx.doi.org/10.1021/jp2104402 | J. Phys. Chem. B 2012, 116, 2831–2841

Table 8. Water−Water Hydrogen Bond Properties and Dynamics[a]

system	n_{HB}^{I} (E_{HB}^{I})	n_{HB}^{II} (E_{HB}^{II})	n_{HB}^{III} (E_{HB}^{III})	τ_{HB}^{I}	τ_{HB}^{II}	τ_{HB}^{III}
$S_{UA,1}$	3.62 (−19.69)	3.76 (−19.53)	3.78 (−18.74)	1.42	1.50	1.38
$S_{UA,2}$	2.73 (−19.50)	2.90 (−19.66)	2.88 (−18.83)	1.61	1.57	1.57
$S_{UA,3}$	3.25 (−20.24)	3.35 (−19.87)	3.43 (−19.28)	1.90	1.93	1.88
$S_{UA,4}$	2.51 (−20.15)	2.60 (−19.93)	2.51 (−19.27)	1.85	1.91	2.04
$S_{AA,1}$	3.59 (−19.60)	3.72 (−19.70)	3.75 (−18.77)	1.50	1.45	1.39
$S_{AA,2}$	2.87 (−19.68)	3.01 (−19.62)	2.88 (−19.03)	1.59	1.59	1.60
$S_{AA,3}$	3.18 (−20.31)	3.28 (−20.35)	3.37 (−19.45)	1.98	1.97	1.99
$S_{AA,4}$	2.70 (−20.64)	2.84 (−20.04)	2.74 (−19.54)	1.95	1.98	2.09

[a] n_{HB}, E_{HB}, and τ_{HB} represent the average number of water−water hydrogen bonds, the energy of the hydrogen bond (in kJ/mol), and the lifetime (in ps), respectively. Regions I, II, and III are defined in the text.

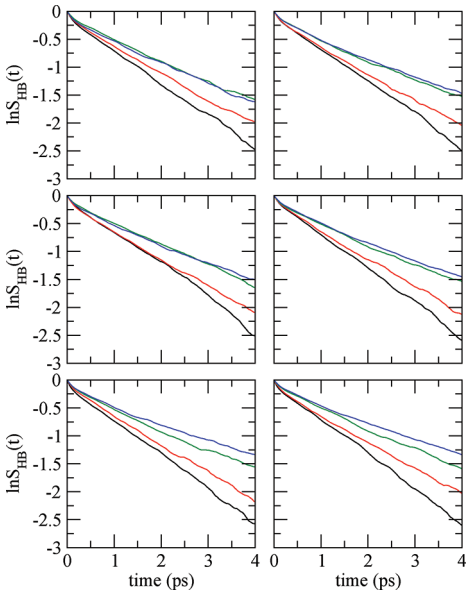

Figure 9. Time dependence of the continuous water−water hydrogen bond correlation function $S_{HB}(t)$ for Regions I, II, and III (from top to bottom, respectively) in water (black), aqueous urea (red), aqueous TMAO (green), and mixed urea/TMAO (blue) solutions. The left panel is for the UA model of methane, and the right panel is for the AA model. Regions I, II, and III are defined in the text.

coordinated water molecules while increasing the number of two and three coordinated water molecules. The comparatively large enhancement of two coordinated water molecules and the reduction of four coordinated water molecules are clearly related to the number of osmolytes that has to be accommodated in the cavities of water molecules. Of significant importance is the number of three coordinated water molecules which do not show any dependence on the number of osmolyte molecules. What we assume is that the central water molecule of these three-coordinated water molecules acts as a hydrogen

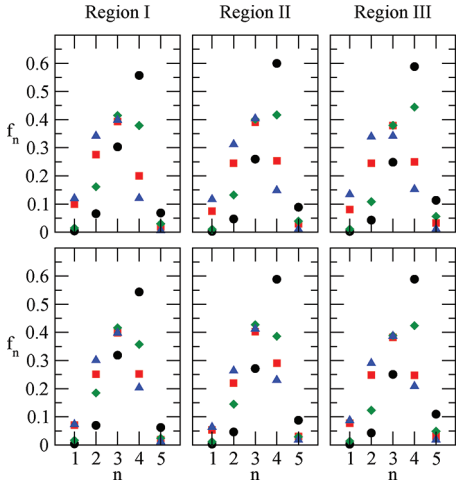

Figure 10. Fraction of molecules with n numbers of water−water hydrogen bonds in different spherical shells around methane in water (○), aqueous urea (□), aqueous TMAO (◇), and mixed urea/TMAO (△) solutions. The top panel is for the UA model of methane, and the bottom panel is for the AA model. Regions I, II, and III are defined in the text.

donor to the osmolyte. A relation of these findings with the hydration of methane can then be imagined in which water solvates urea and TMAO (mainly through hydrogen bonds) and at the same time increases the water−water hydrogen bond lifetime, thereby making itself less available to solvate hydrophobic groups, which is consistent with our coordination number analysis showing the dehydration of methane in aqueous osmolyte solutions.

IV. SUMMARY AND CONCLUSIONS

In this article, we have investigated hydrophobic interactions of methane and also the structure of the solution in the presence and absence of two naturally occurring osmolytes, urea and TMAO. We considered two different methane models, namely, united atom (UA) and all site models (AA). From the PMF plots we find that they behave very similarly both in pure water and in aqueous osmolyte solutions except for the binary aqueous solution of AA model containing urea molecules where we observe urea-induced enhancement of methane association. This is further confirmed by our association constant calculations and cluster structure analyses. Our preferential interaction calculations show that in binary aqueous urea solution methane molecules prefer to interact more with water molecules over urea molecules. Supplementary to the earlier studies,[20,21] our results show that methane molecules are expelled by urea molecules which enhances the local concentration of methane molecules leading to the association of methane. In binary aqueous urea solution, this preferential binding of urea molecules with solute is lower for the all site methane model compared to that for united atom model. As a result, expelling more methane molecules by urea molecules for the all site model takes place, leading to more association of it, and this is reflected in the well depth of CM in the PMF plots and in the association constant values. In binary aqueous TMAO solution, in its solvation shell, methane molecules interact preferentially with TMAO molecules. But, contrary to as one would expect, our association constant calculations and cluster structure analyses did not show any noticeable influence of TMAO molecules on methane−methane interactions. This is, probably, due to the fact that methane molecules act as a "substitute" for the methyl groups of TMAO molecules. So, the

dx.doi.org/10.1021/jp2104402 | J. Phys. Chem. B 2012, 116, 2831−2841

presence of methyl groups in TMAO helps to associate methane molecules as well as reduce the hydrophobic effect between methane molecules. These two opposing effects nullify the effects of each other leading to negligible effects of TMAO on methane aggregation. Again, since, the size of a methane molecule in both models is comparable and both models interact with solvent and cosolvent molecules in similar fashion, we observe that these two models behave very similarly both in water and in aqueous solutions containing osmolytes. This is reflected in our structural properties calculations such as different solute−solvent distribution functions and in coordination number analyses studies.

The water orientational profile calculations suggest that the orientation of water molecules near to hydrophobic surface is anisotropic. The dipole vector of a water molecule in this region oscillates between 55 and 124° with the unit vector. As we move further away from the solute surface, this distribution becomes flatter, and as expected, there is no preferred orientation of water molecules at the bulk region. Only a slight change in the orientational profiles of water is observed in the presence of osmolytes.

Our hydrogen-bond properties calculations in different layers around the solute molecule show that the average number of water−water hydrogen bonds remains practically unchanged in different layers. This is due to the fact that smaller methane molecules can easily fit into the cavities generated by normal fluctuations in the solvent density, keeping average number of water−water hydrogen bonds unchanged. Nonetheless, water loses some of its identical nearest neighbors in the vicinity of the hydrophobic solute, in excellent agreement with the observation of Meng and Kollman[49] that water molecules in the hydration shell of methane participate in the same average number of hydrogen bonds as water in the bulk but have a reduced number of nearest neighbor water molecules. We also find a negligible change in the lifetime of water−water hydrogen bonds in the vicinity of methane as compared to the bulk region. In aqueous solutions of osmolyte, the number of four and five coordinated water molecules decreases with corresponding increase in two and three coordinated water molecules. The average number of water−water hydrogen bonds seems to be influenced by the number of osmolyte molecules that enter into the water cavities. On the addition of TMAO molecules there is a profound increase in the hydrogen bond lifetime as reported previously by Bennion et al.[2] A direct hydrogen bonding interaction of TMAO with both water and urea is also observed. In the context of the counteraction effect of TMAO molecules on urea-induced protein denaturation, our results imply that the solvation of TMAO by water and urea molecules along with TMAO induced strengthening of water−water hydrogen bonds do not affect the hydrophobic interaction of nonpolar moieties. But these could be the important factors in reducing the solvation of the protein backbone by water and urea and hence countering the urea-induced denaturation of protein.

AUTHOR INFORMATION

Corresponding Author

*E-mail address: sandipp@iitg.ernet.in.

Notes

The authors declare no competing financial interest.

ACKNOWLEDGMENTS

The financial support of DST, Govt. of India is gratefully acknowledged. The author R.S. thanks CSIR, India for providing JRF fellowship.

REFERENCES

(1) Daggett, V. *Chem. Rev.* **2006**, *106*, 1898 ; and references therein.
(2) Bennion, B. J.; Daggett, V. *Proc. Natl. Acad. Sci.* **2004**, *101*, 6433.
(3) Venkatesu, P.; Lee, M.-J.; Lin, H.-m. *J. Phys. Chem. B* **2009**, *113*, 5327.
(4) Mukherjee, A.; Santra, M. K.; Beuria, T. K.; Panda, D. *FEBS J.* **2005**, *272*, 2760.
(5) Yancey, P. H.; Somero, G. N. *J. Exp. Zool.* **1980**, *212*, 205.
(6) Yancey, P. H. *J. Exp. Biol.* **2005**, *208*, 2819.
(7) Bennion, B. J.; Daggett, V. *Proc. Natl. Acad. Sci.* **2003**, *100*, 5142.
(8) Caballero-Herrera, A.; Nordstrand, K.; Berndt, K. D.; Nilsson, L. *Biophys. J.* **2005**, *89*, 842.
(9) Mountain, R. D.; Thirumalai, D. *J. Am. Chem. Soc.* **2003**, *125*, 1950.
(10) Tanford, C. *J. Am. Chem. Soc.* **1964**, *86*, 2050.
(11) Finer, E. G.; Franks, F.; Tait, M. J. *J. Am. Chem. Soc.* **1972**, *94*, 4424.
(12) Wei, H.; Fan, Y.; Gao, Y. Q. *J. Phys. Chem. B* **2010**, *114*, 557.
(13) Yang, L.; Gao, Y. Q. *J. Am. Chem. Soc.* **2010**, *132*, 842.
(14) Paul, S.; Patey, G. N. *J. Am. Chem. Soc.* **2007**, *129*, 4476.
(15) Zou, Q.; Bennion, B. J.; Daggett, V.; Murphy, K. P. *J. Am. Chem. Soc.* **2002**, *124*, 1192.
(16) Meersman, F.; Bowron, D.; Soper, A. K.; Koch, M. H. J. *Biophys. J.* **2009**, *97*, 2559.
(17) Wallqvist, A.; Covell, D. G.; Thirumalai, D. *J. Am. Chem. Soc.* **1998**, *120*, 427.
(18) Alonso, D. O.; Dill, K. A. *Biochemistry* **1991**, *30*, 5974.
(19) Ikeguchi, M.; Nakamura, S.; Shimizu, K. *J. Am. Chem. Soc.* **2001**, *123*, 677.
(20) Trzesniak, D.; Van der Vegt, N. F. A.; Van Gunsteren, W. F. *Phys. Chem. Chem. Phys.* **2004**, *6*, 697.
(21) Oostenbrink, C.; Van Gunsteren, W. F. *Phys. Chem. Chem. Phys.* **2005**, *7*, 53.
(22) Lee, M.-E.; Van der Vegt, N. F. A. *J. Am. Chem. Soc.* **2006**, *128*, 4948.
(23) Zangi, R.; Zhou, R.; Berne, B. J. *J. Am. Chem. Soc.* **2009**, *131*, 1535.
(24) Athawale, M. V.; Dordick, J. S.; Garde, S. *Biophys. J.* **2005**, *89*, 858.
(25) Paul, S.; Patey, G. N. *J. Phys. Chem. B* **2007**, *111*, 7932.
(26) Paul, S.; Patey, G. N. *J. Phys. Chem. B* **2008**, *112*, 11106.
(27) Pratt, L. R.; Chandler, D. *J. Chem. Phys.* **1980**, *73*, 3430.
(28) Lum., K.; Chandler, D.; Weeks, J. D. *J. Phys. Chem. B* **1999**, *103*, 4570.
(29) Rajamani, S.; Truskett, T. M.; Garde, S. *Proc. Natl. Acad. Sci.* **2005**, *102*, 9475.
(30) Athawale, M. V.; Goel, G.; Ghosh, T.; Truskett, T. M.; Garde, S. *Proc. Natl. Acad. Sci.* **2007**, *104*, 733.
(31) Berendsen, H. J. C.; Grigera, J. R.; Straatsma, T. P. *J. Phys. Chem.* **1987**, *91*, 6269.
(32) Duffy, E. M.; Severance, D. L.; Jorgensen, W. L. *Isr. J. Chem.* **1993**, *33*, 323.
(33) Kast, K. M.; Brickmann, J.; Kast, S. M.; Berry, R. S. R. *J. Phys. Chem. A* **2003**, *107*, 5342.
(34) Jorgensen, W. L.; Tirado-Rives, J. *J. Am. Chem. Soc.* **1988**, *110*, 1657.
(35) Stassen, H. *J. Mol. Struct.: THEOCHEM* **1999**, *464*, 107.
(36) Allen, M. P.; Tildesley, D. J. *Computer Simulation of Liquids*; Oxford University Press: New York, 1987.
(37) Martinez, H. L.; Ravi, R.; Tucker, S. C. *J. Chem. Phys.* **1996**, *104*, 1067.
(38) Kokubo, H.; Pettitt, B. M. *J. Phys. Chem. B* **2007**, *111*, 5233.
(39) Pagnotta, S. E.; Ricci, M. A.; Bruni, F.; McLain, S.; Magazu, S. *Chem. Phys.* **2008**, *345*, 159.
(40) Ben-Naim, A. *J. Phys. Chem.* **1989**, *93*, 3809.
(41) Mancera, R. L.; Buckingham, A. D.; Skipper, N. T. *J. Chem. Soc., Faraday Trans.* **1997**, *93* (13), 2263.
(42) Garde, S.; Hummer, G.; Paulaitis, M. E. *Faraday Discuss.* **1996**, *103*, 125.

(43) Garde, S.; Hummer, G.; Paulaitis, M. E. *J. Chem. Phys.* **1998**, *108*, 1552.
(44) Rajamani, S.; Ghosh, T.; Garde, S. *J. Chem. Phys.* **2004**, *120*, 4457.
(45) Paul, S.; Chandra, A. *J. Chem. Phys.* **2005**, *123*, 184706.
(46) Lee, C. Y.; McCammon, J. A.; Rossky, P. J. *J. Chem. Phys.* **1984**, *80*, 4448.
(47) Paul, S.; Chandra, A. *J. Phys. Chem. B* **2005**, *109*, 20558.
(48) Paul, S.; Chandra, A. *J. Chem. Theor. Comput.* **2005**, *1*, 1221.
(49) Meng, E. C.; Kollman, P. A. *J. Phys. Chem.* **1996**, *100*, 11460.